



OPEN Clinical safety and efficacy of elliptical thin-flap LASIK using a low-pulse energy femtosecond laser

Hung-Yuan Lin¹, Ya-Jung Chuang^{2✉}, Steven Wei-Hsin Chang³ & Pi-Jung Lin⁴

This study assessed the clinical safety and efficacy of elliptical thin-flap LASIK with a low-pulse energy femtosecond laser in 3 thickness subgroups (85, 90, and 100 μm). A total of 80 patients who underwent bilateral LASIK surgery at Taiwan between April and September 2019 were retrospectively enrolled. Elliptical corneal flaps with wide temporal hinges and inverted-angled side cuts were created. Target flap thickness was calculated on the basis of residual stromal bed thickness and percent tissue altered. Before flap creation, an optical coherence tomography image for visualization of the pre-cut flap position was obtained with the built-in camera. At postoperative month 1, the overall mean logMAR uncorrected distance visual acuity (UDVA) was -0.04 ± 0.07 (20/18 Snellen), with 96% of eyes achieving UDVA of 20/20 or better. Postoperative mean manifest spherical equivalent was -0.37 ± 0.42 D at 1 month. The visual and refractive outcomes in each of the 3 subgroups were similar. The achieved flap thicknesses were found to be highly predictable and consistent in the respective thickness subgroups. Optical coherence tomography-guided thin-flap LASIK performed with the low-pulse energy femtosecond laser was found to be safe with no intraoperative or postoperative complications.

Laser in situ keratomileusis (LASIK), one of the most commonly and successfully performed refractive procedures, is known for being a safe procedure that allows for consistently good visual outcomes and rapid vision recovery^{1–3}. Flap creation is an important step during the first phase of the procedure for the correction of ametropia because flap thickness varies depending on the technique and device used⁴. Traditionally, flaps range in thickness between 100 and 160 μm ^{5,6}. The use of femtosecond instead of microkeratome lasers for flap creation has become more common in recent years^{7,8}. Femtosecond lasers are safe and allow for precise and consistent flap creation^{6,7,9}. This is important because the flap thickness has a direct influence on residual stromal bed thickness (RSBT), consequently affecting the safety of the procedure⁹. Iatrogenic ectasia is the most feared complication encountered after LASIK. Insufficient RSBT is a major risk factor for post-LASIK ectasia¹⁰. Therefore, surgical practice has further transitioned from the conventional creation of thick flaps to the creation of thin flaps to preserve RSBT and reduce the risk of ectasia. However, thin flaps are a risk factor for several complications, such as buttonhole, flap striae, epithelial ingrowth, irregular astigmatism, and flap tear^{6,11–14}. Given the advantage thin flaps offer in preserving RSBT, strategies that enable the safe creation of thin flaps should be identified.

A literature review revealed that preserving flap integrity reduces the risk of flap striae¹⁵. Elliptical flaps with a wide hinge angle and inverted side-cut angle have been associated with improved biomechanical performance and flap integrity^{16–19}. Flaps created with femtosecond lasers have planar morphologies that improve adhesion to the underlying stromata^{15,20}. In addition, femtosecond lasers that use low pulse energy minimize cavitation bubbles, which in turn reduces the potential for opaque bubble layer and other gas bubble-related complications²¹.

The cutting process of the FEMTO LDV Z8 femtosecond laser (Ziemer Group AG, Switzerland) follows a specific sequence. First, venting channels are created (optional selection). Second, the stromal cut is made, and last, the side cut is made. The FEMTO LDV Z8 laser has high numerical aperture optics. Its strongly focused beam irradiates the cornea with very small overlapping spots ($< 2 \mu\text{m}$ in diameter), and it uses low pulse energy (in the nJ range)²². The overlapping spots create a smooth cleavage plane, and this reduces the possibility of

¹Universal Eye Center, Zhong-Li, Taoyuan City 320066, Taiwan (R.O.C.). ²Universal Eye Center, Long-Tan, No. 483, Yanping Rd., Zhongli Dist., Taoyuan City 320066, Taiwan (R.O.C.). ³Department of Biomedical Engineering, I-Shou University, Kao-hsiung City 840301, Taiwan (R.O.C.). ⁴Universal Eye Center, Da'an Dist., Taipei City 106021, Taiwan (R.O.C.). ✉email: rannyposh@gmail.com

tissue bridges across the interface, thereby facilitating easy flap lifting²³. Since the duration of laser pulses is in the femtosecond range, the process of photodisruption is induced at the beam focus. Plasma generated at the focus causes immediate evaporation of the tissue. Spatially overlapping plasma regions of subsequent laser pulses gently and efficiently separate the tissue without the need for mechanical effects like tearing of tissue by cavitation bubbles²⁴. Gas generation during cutting is minimized due to the use of low pulse energy, and an optimized cutting sequence further reduces the risk of opaque bubble layer complications. The thickness of a flap created by the FEMTO LDV Z8 laser can be controlled precisely²⁵.

In the present retrospective study, the low-pulse-energy FEMTO LDV Z8 femtosecond laser was used to create elliptical flaps of different thicknesses ranging from 80 to 100 μm with a wide temporal hinge and inverted-angle side cut. The purpose of this study was to evaluate the visual outcomes of LASIK using different flap thicknesses (80–100 μm) created with the same laser and to describe any complications.

Methods

This retrospective study included the anonymized data of 80 myopic patients (160 eyes) who underwent bilateral LASIK at the Universal Eye Center in Zhongli, Taiwan, between April and September 2019 and who completed the 1-month follow-up visit. By including consecutive eyes that met the inclusion criteria, we aimed to minimize selection bias and enhance the reliability of our outcomes. The study was conducted in accordance with the tenets of the Declaration of Helsinki and its amendments, and it was approved by the Institutional Review Board (IRB) of Antai Tian-Sheng Memorial Hospital (IRB 19-082-B). As part of routine clinical protocol, written informed consent for LASIK was obtained from all patients. However, informed consent specific to this study was waived by the ethics committee of the hospital, as the data were collected during normal care provision.

Eligibility criteria

The study included patients aged 19–50 years. Patients were included if they had moderate-to-high myopia (from -3.00 to -11.00 D), astigmatism or no astigmatism (up to -6.00 D), stable refractive error for at least 12 months, central corneal thickness (CCT) of > 480 μm , estimated RSBT of > 300 μm , and normal keratometry and topography readings. Exclusion criteria included evidence of keratoconus or forme fruste keratoconus, high risk of post-LASIK ectasia, prior corneal surgery or retinal disease, the presence of active ocular or systemic pathologies that could affect corneal health, and the presence of moderate-to-severe dry eye.

Preoperative examination

All patients underwent a complete preoperative ophthalmologic examination that included assessment of uncorrected distance visual acuity (UDVA), best-corrected distance visual acuity (CDVA), manifest and cycloplegic refraction, slit lamp examination, Schirmer's test, white-to-white diameter, dilated fundus evaluation, intraocular pressure, and CCT (using a Lenstar LS900 Pentacam; Oculus Inc.). Furthermore, patients underwent tomography screening for keratoconus (Pentacam; Oculus Inc.) and topography screening (OPD Scan III Nidek).

The target flap thickness (FT) was based on the predicted RSBT and percent tissue altered (PTA). RSBT was calculated by subtracting the target FT and ablation depth (AD) from the CCT:

$$\text{RSBT} = \text{CCT} - \text{FT} - \text{AD}$$

The maximum AD was kept at < 150 μm . PTA was based on the following formula for LASIK using FT, AD, and CCT:

$$\text{PTA} = (\text{FT} + \text{AD}) / \text{CCT}$$

PTA values $\geq 40\%$ indicate a risk for ectasia.

Based on the calculations of RSBT and PTA, the most suitable target FTs were 80, 85, 90, 95, and 100 μm (80 to 100 μm).

Surgical technique

All procedures were performed under topical anesthesia by surgeons (H-Y Lin, and Y-J Chuang) skilled in handling thin flaps. The FEMTO LDV Z8 laser was used to create flaps of thicknesses between 80 and 100 μm . An elliptical flap with a horizontal diameter of either 9.0–8.55 mm and a temporally positioned hinge of 0.6 mm was created. The suction ring was centered and docked, and suction was applied. Before flap creation, an optical coherence tomography (OCT) scan (Fig. 1) was performed as an extra safety measure to visualize the precut flap position to ensure that the flap was placed below the Bowman layer. Suction was turned off automatically after the flap was created. In this study, a WaveLight EX-500 (Alcon Laboratories, Inc., Fort Worth, TX, USA) excimer laser was used to perform the refractive procedure. After ablation, the stromal bed was irrigated with a balanced salt solution, and the elliptical flap floated back into its original position. The flap was checked for proper adherence in the slit lamp without contact lens wearing.

Postoperative management

All patients were examined 30 min after surgery to check for correct flap positioning and the presence of interface debris in the slit lamp again.

Postoperatively, TobraDex eye drops (Alcon) were instilled qid for 1 week. After discontinuation of TobraDex, Flumetholon 0.02% (Fuorometholone, Santen) was prescribed for 3 weeks. A 1–2-month supply of artificial tears was prescribed.

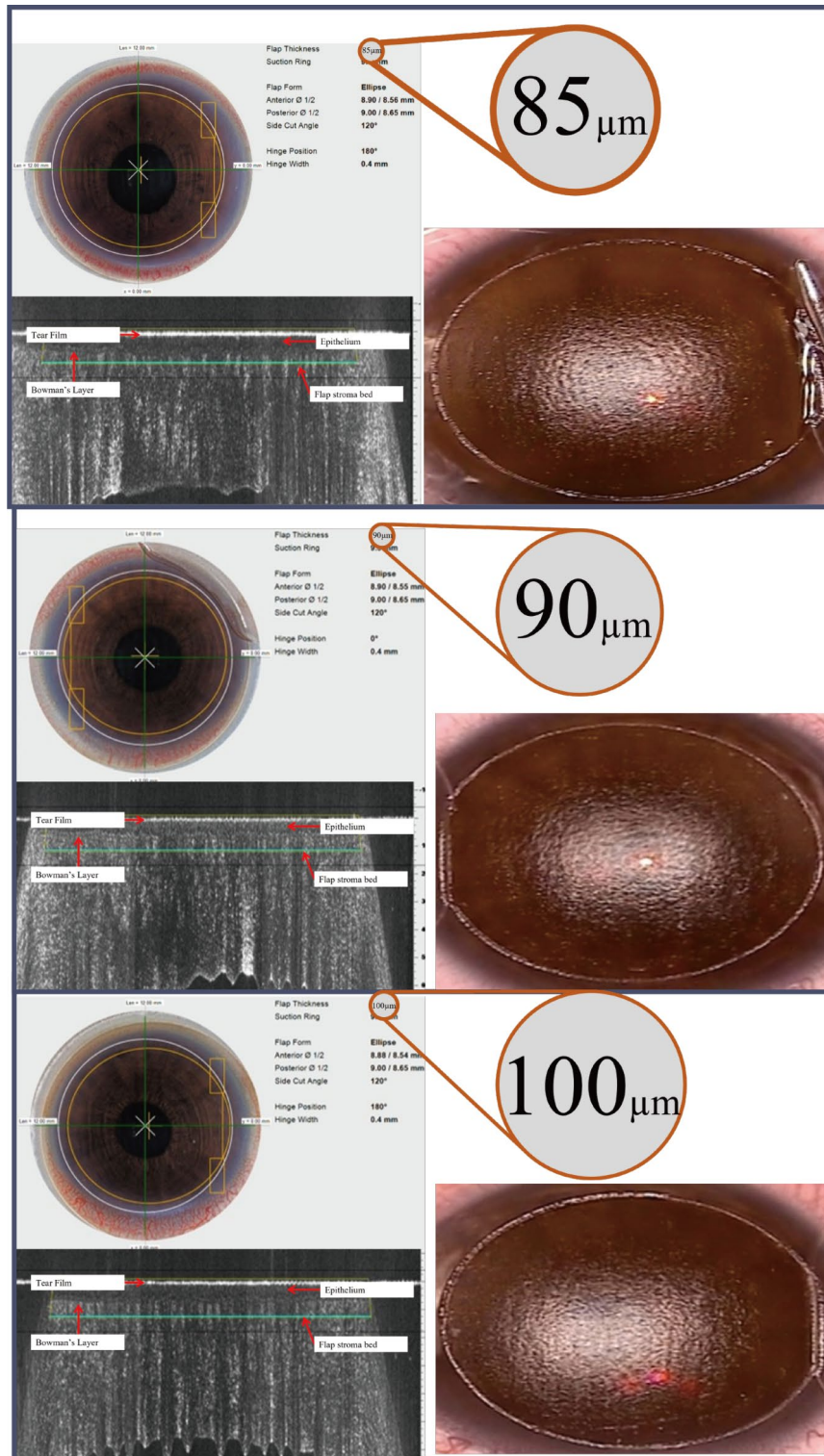


Fig. 1. FEMTO LDV Z8 build in OCT image showing epithelium and cut being placed stroma layer.

Postoperative examination

Patients were examined at follow-up visits 1 day, 1 week, 2 weeks, and 1 month after the procedure. Assessments at each visit included UDVA, CDVA, keratometry, manifest, and slit lamp examination. Flap thickness was measured using OCT (Spectralis OCT, Heidelberg Engineering, Germany) at postoperative day 1.

Statistical analysis

Statistical analyses were performed using SAS software (version 9.4, SAS Institute, Inc., Cary, NC, USA). Snellen’s visual acuity was converted to the logarithm of the minimum angle of resolution (logMAR) for statistical analysis. Subgroup analysis was performed by categorizing the patients on the basis of target flap thickness (85, 90, and 100 μm). Subgroup analysis of the 80 and 95 μm subgroups was not performed due to inadequate sample size (≤ 2). A *p* value of < 0.05 was considered statistically significant.

Results

This study included 160 eyes and 80 patients (53.8% male and 46.3% female). The mean (\pm SD) age of patients was 31.4 ± 6.9 years (range: 19–47 years). The mean (\pm SD) CCT was 556.04 ± 31.04 μm. Subgroup analysis was performed by categorizing the patients into 3 subgroups based on target flap thickness. Subgroup analysis included 95 patients (85-μm subgroup), 18 patients (90-μm subgroup), and 44 patients (100-μm subgroup).

Visual outcomes

Overall mean UDVA improved significantly ($p < .0001$) from 1.19 ± 0.21 logMAR (20/310 Snellen) preoperatively to -0.04 ± 0.07 logMAR (20/18 Snellen) postoperatively. The mean postoperative logMAR UDVA was similar among the 85-μm (-0.04 ± 0.07), 90-μm (-0.05 ± 0.04), and 100-μm (-0.04 ± 0.10) subgroups. In total, 156 eyes were targeted for emmetropia. When analyzing UDVA outcomes, 4 eyes were excluded due to monovision. At the 1-month follow-up visit, 96% of eyes achieved a UDVA of 20/20 or better (Fig. 2a). Corresponding

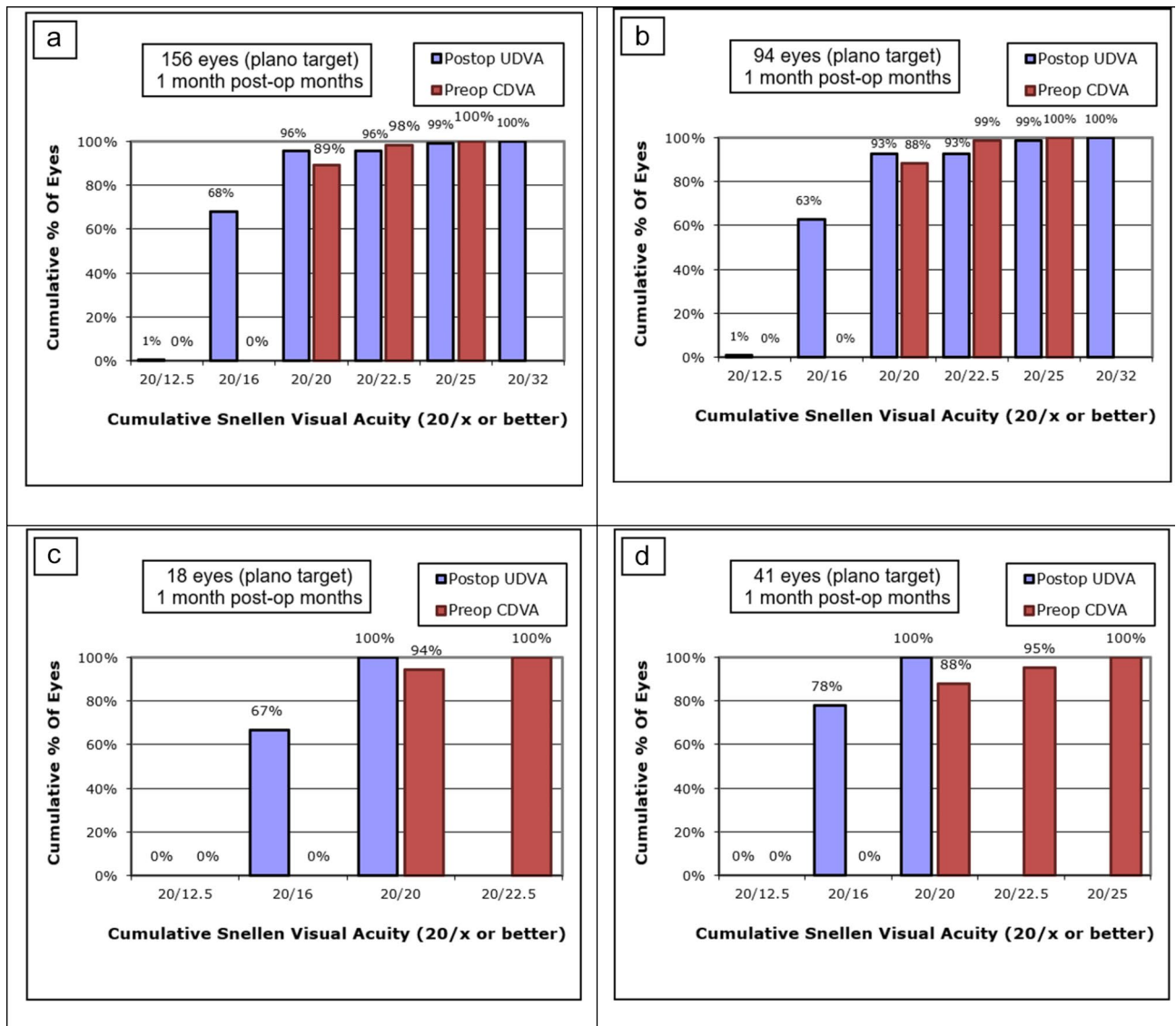


Fig. 2. Uncorrected Visual Acuity (UDVA) and Corrected Visual Acuity (CDVA) at 1 month postoperative follow up visit. (a) overall cohort, (b) 85 μm flap thickness group, (c) 90 μm flap thickness group, (d) 100 μm flap thickness group.

results were comparable for the 3 subgroups (93%, 100%, and 100% for the 85-, 90-, and 100- μ m subgroups, respectively; Fig. 2b–d).

Postoperatively, the overall mean logMAR CDVA was -0.05 ± 0.04 (20/20 Snellen). Similar results were achieved for the 85- (-0.05 ± 0.05), 90- (-0.06 ± 0.04), and 100- μ m (-0.06 ± 0.03) subgroups. There was a gain of 1 or more lines of CDVA in 73% of eyes, and 26% of eyes showed no change. Loss of 2 or more lines of CDVA was observed in 0.6% of eyes (Fig. 3a). Corresponding results for the loss of 2 or more lines of CDVA were 1.1%, 0%, and 0% for the 85-, 90-, and 100- μ m subgroups, respectively (Fig. 3b–d). Loss of 2 or more lines was observed in only 1 eye; this was due to diffuse superficial punctate keratitis.

Overall, the safety and efficacy indices were 1.13 ± 0.16 and 1.15 ± 0.12 , respectively. The values for the safety and efficacy indices were found to be consistent among the 85- (1.14 ± 0.13 , 1.12 ± 0.15), 90- (1.15 ± 0.09 , 1.14 ± 0.09), and 100- μ m (1.18 ± 0.10 , 1.14 ± 0.09) subgroups.

Refractive outcomes

The scatterplot of achieved versus attempted manifest spherical equivalent at 1 month revealed an R^2 value of 0.9684, which indicates low scatter (Fig. 4a). Similar R^2 values were obtained for the 3 subgroups (Fig. 4b, c and d). The mean manifest spherical equivalent improved from -5.41 ± 2.10 D preoperatively to -0.37 ± 0.42 D postoperatively. At 1 month, 69% and 91% of eyes achieved manifest spherical equivalent within ± 0.50 D and ± 1.00 D of target correction (Fig. 5a). The percentage of eyes within ± 0.50 D and ± 1.00 D were comparable among the 85-, 90-, and 100- μ m subgroups (Fig. 5b–d).

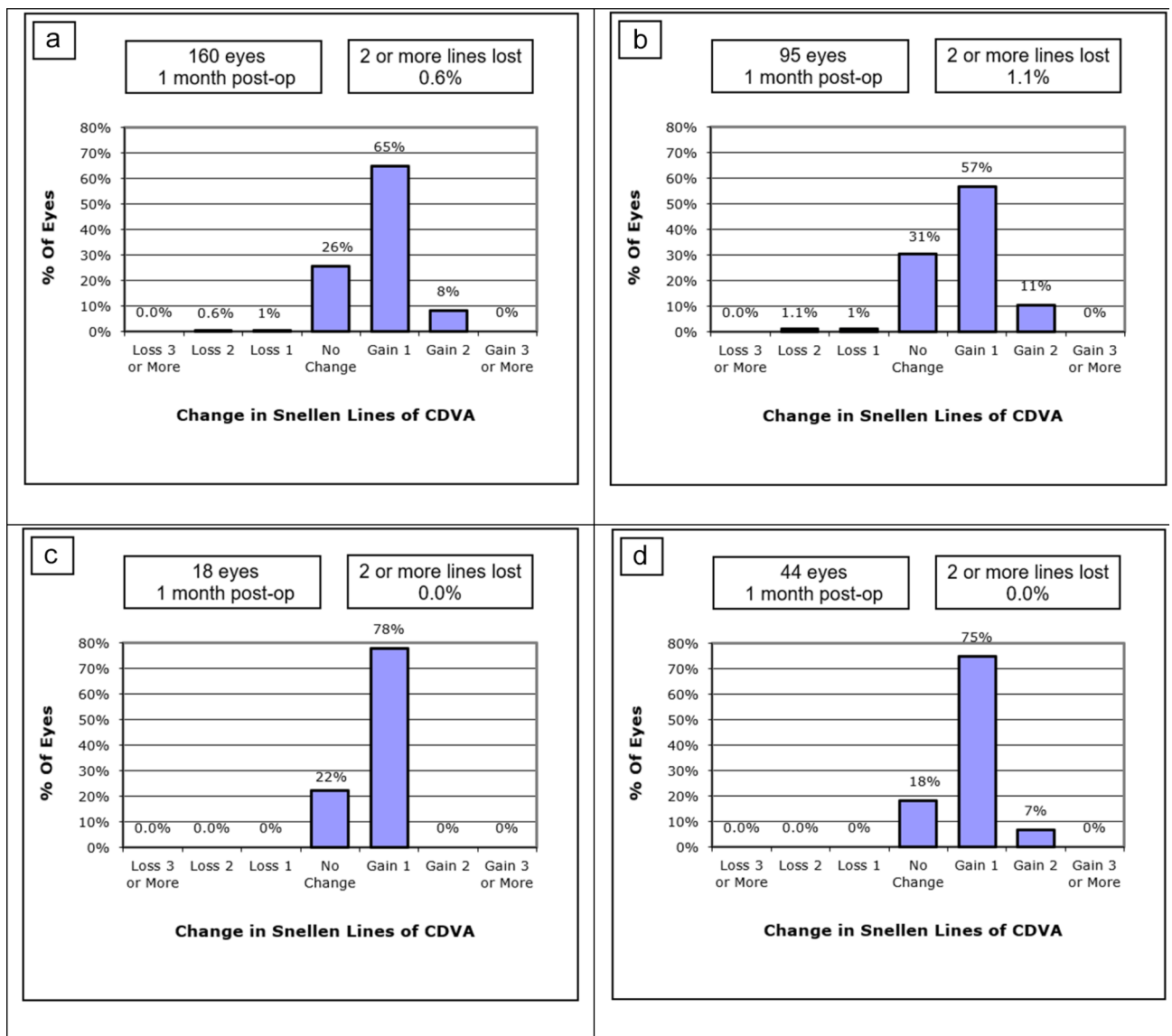


Fig. 3. Change in snellen lines of CDVA at 1-month postoperative follow up visit. (a) overall cohort, (b) 85 μ m flap thickness group, (c) 90 μ m flap thickness group, (d) 100 μ m flap thickness group.

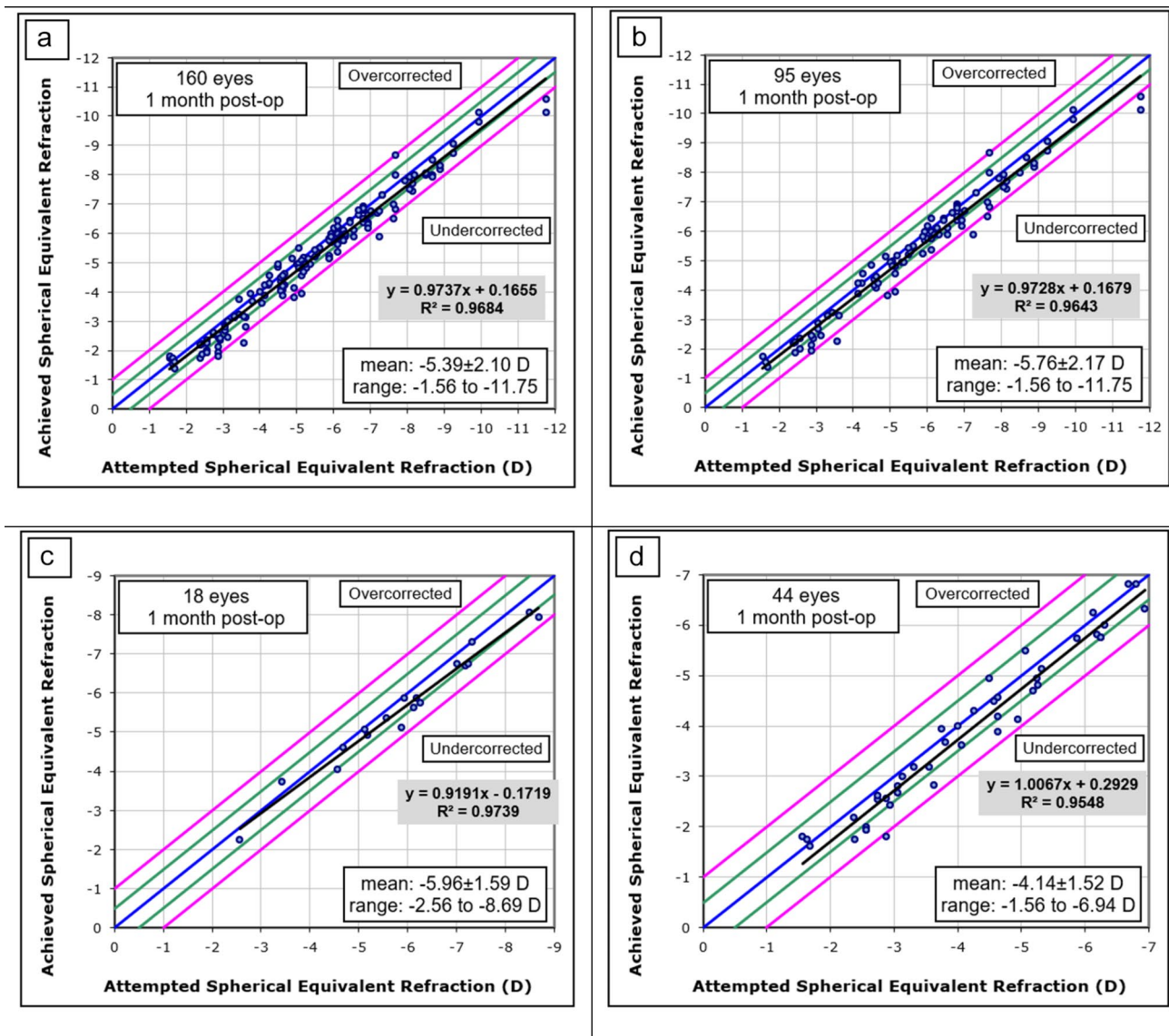


Fig. 4. Attempted versus achieved manifest refraction spherical equivalent at 1-month postoperative follow up visit. **(a)** overall cohort, **(b)** 85 μ m flap thickness group, **(c)** 90 μ m flap thickness group, **(d)** 100 μ m flap thickness group.

Refractive astigmatism

At the 1-month follow-up visit, 75% of eyes had a residual cylinder within 0.50 D, and 99% were within 1.00 D (Fig. 6a). The percentage of eyes with a residual cylinder within 0.50 D and 1.00 D was similar in the 85-, 90-, and 100- μ m subgroups (Fig. 6b–d).

Target and achieved flap thickness

In all 3 subgroups, the mean flap thickness achieved was close to the target flap thickness. The achieved flap thickness was 84.60 ± 0.93 μ m for the target flap thickness of 85 μ m; 89.43 ± 0.51 μ m for the target flap thickness of 90 μ m, and 99.82 ± 0.46 μ m for the target flap thickness of 100 μ m.

Complications

No clinically relevant complications occurred intraoperatively or postoperatively in any of the patients.

Discussion

This retrospective study assessed the clinical safety and efficacy of thin-flap LASIK with flaps ranging in thickness between 80 and 100 μ m. A low-pulse-energy femtosecond laser was used to create elliptically shaped flaps with a temporal hinge and inverted side cut. Study results suggest that the visual and refractive outcomes for each of the flap thickness subgroups were comparable at a 1-month follow-up visit in terms of efficacy, safety,

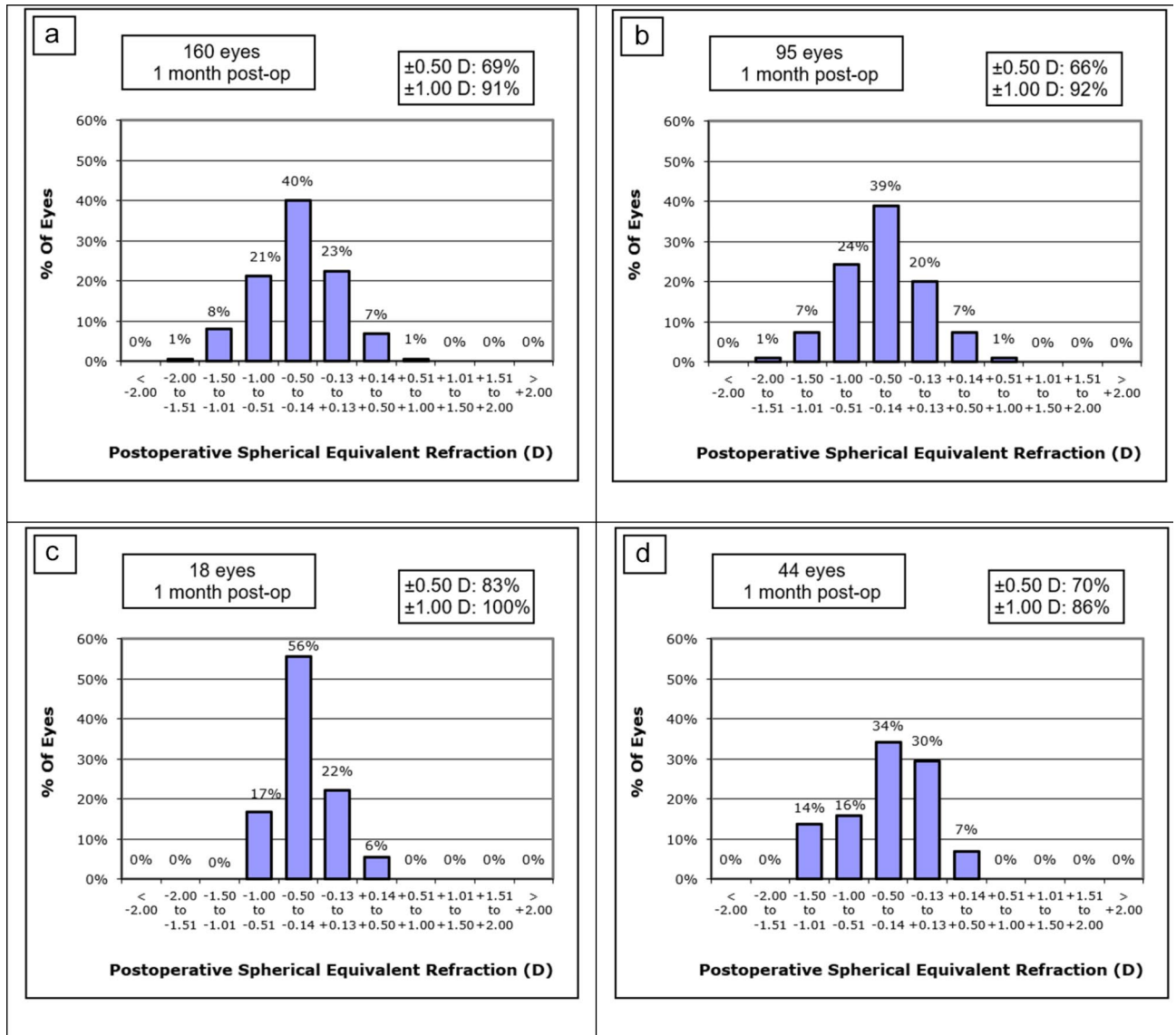


Fig. 5. Percentage of eyes with postoperative manifest refraction spherical equivalent between ± 0.50 D and ± 1.00 D at 1-month postoperative follow up visit. (a) overall cohort, (b) 85 μm flap thickness group, (c) 90 μm flap thickness group, (d) 100 μm flap thickness group.

predictability, refractive accuracy, and refractive astigmatism. No intraoperative or postoperative complications, such as opaque bubble layer, flap striae, or buttonholes, were observed.

Cumulatively, excellent efficacy (96% of eyes with a UDVA of 20/20 or better) with a good correlation between the attempted versus achieved spherical equivalent was obtained at the 1-month follow-up visit. The results were comparable to a previous study on thin-flap (80/90 μm) LASIK¹². The efficacy and safety indices were consistent among the 85-, 90-, and 100- μm subgroups, with overall mean efficacy and safety indices of 1.13 and 1.15, respectively. While no loss of CDVA was observed among eyes in the 90- and 100- μm subgroups, a loss of CDVA in 2 eyes in the 85- μm subgroup (Fig. 2b) was found to be due to diffuse superficial punctate keratitis observed 1 month postoperatively. Fortunately, after dry eye management, uncorrected visual acuity was restored to 20/20 in both eyes between the 2-month and 1-year follow-up visits.

Consistency and predictability of corneal flap thickness are crucial for surgical planning and for yielding desirable LASIK outcomes. The low-pulse-energy laser has been shown to produce thin flaps with good depth predictability⁶. In a recent study presented at the 2021 European Society of Cataract and Refractive Surgeons congress in Amsterdam, the 1-month follow-up results of 2-dimensional versus 3-dimensional flaps of 110- μm thickness created with the FEMTO LDV Z8 laser were compared. Achieved flap thicknesses were 110.67 ± 1.60 and 111.21 ± 1.65 μm for the 2-dimensional and 3-dimensional groups, respectively, showing good predictability²⁵. Likewise, in the present study, flap thickness was found to have excellent predictability. In all subgroups, the mean achieved corneal thickness was close to the target flap thickness. We measured corneal flap thickness using OCT on postoperative day 1. It is acknowledged that flap edema on the first day post-procedure

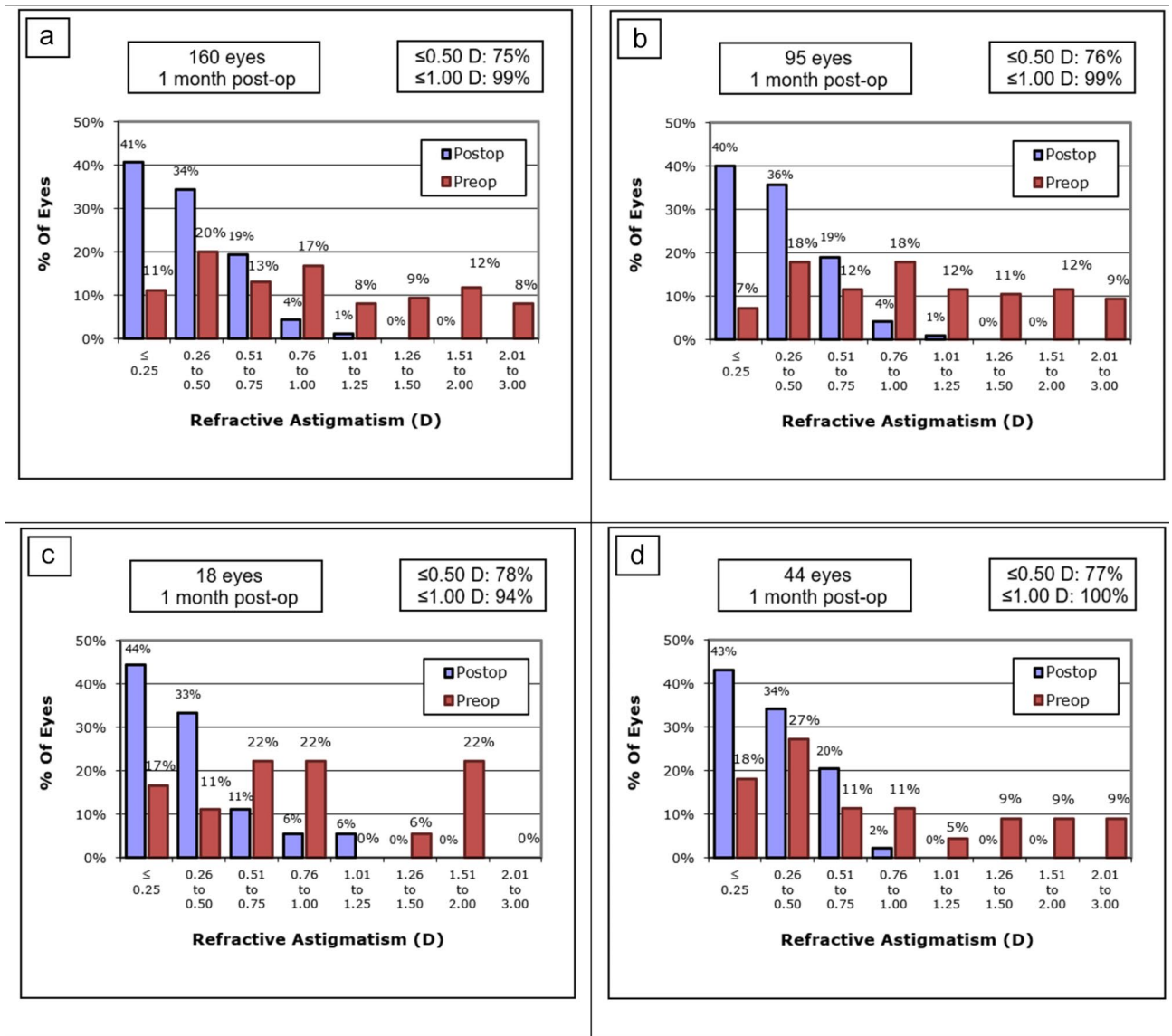


Fig. 6. Percentage of eyes with postoperative refractive astigmatism between ± 0.50 D and ± 1.00 D at 1-month postoperative follow up visit. (a) overall cohort, (b) 85 μ m flap thickness group, (c) 90 μ m flap thickness group, (d) 100 μ m flap thickness group.

may affect the accuracy of these measurements. However, as patients did not wear contact lenses and were instructed to rest and use prescribed eye drops properly, we believe the likelihood of corneal edema was very low.

Although thin-flap LASIK can enhance patient safety in terms of preserving the residual bed, these flaps are difficult to handle and are more easily displaced. The thinner and larger the flap is, the more it tends to shift¹¹. This increases the likelihood of various postoperative complications, including the development of flap striae and folds. In addition to flap thickness, other factors contribute to the development of flap striae and folds. For instance, uneven alignment of the flap edge and the peripheral epithelial ring has been found to result in flap folds. The presence of high myopia also increases the risk of flap folds owing to the tenting effect²⁶. Postoperative dry eye resulting from insufficient reflex blinking after surgery, use of topical anesthetic, and cutting of the corneal nerves leaves the corneal surface dry between blinks and more vulnerable to detachment and displacement of the flap. None of the eyes in the present study presented with flap striae. The absence of flap striae could be attributed to flaps being meticulously repositioned, well dehydrated, and smoothed out with a spear sponge after ablation, thereby ensuring proper flap adhesion. Patients in the present study were asked to keep their eyes closed during the early postoperative period. The combination of the oval flap, temporal hinge, and inverted side cut may have contributed to nearly absence of microstriae^{12,13}. Likewise, the increased flap adherence due to the creation of planar flaps might have reduced the risk of epithelial ingrowth¹⁹. In our opinion, the ability of the FEMTO LDV Z8 laser to create cuts with high precision and predictability contributed to the overall absence of postoperative complications.

The results of the present study corroborate the findings of previous studies that reported no flap striae with 80-, 90-, and 100- μm flap thicknesses in 3090 eyes^{12,13}. Another study that evaluated 103 eyes with 90- μm flaps and 27 eyes with 80- μm flaps created using a Ziemer FEMTO LDV femtosecond laser found no striae in the 80- μm group but microstriae in 4 eyes (3.9%) in the 90- μm group⁶. This suggests that factors other than flap thickness may contribute to the development of flap striae and folds.

With thin-flap LASIK, there is an induced risk of intraoperative complications such as pseudobuttonholes. The thinner the flap is, the closer it is to the Bowman layer. Flap buttonholes are caused by an abnormal lamellar cut during the creation of the LASIK flap. In the present study, no buttonholes were observed intraoperatively. This might be attributable to the high predictability of the laser and intraoperative OCT visualization of the pre-cut flap position enabling the creation of flaps of the target flap thicknesses. The built-in OCT camera of the FEMTO LDV Z8 laser allows visualization of the pre-cut flap position to ensure that it is placed correctly (below the Bowman layer; Fig. 1). In addition, the flat appplanation interface might have contributed to a lower rate of intraoperative complications.

High-pulse-energy femtosecond lasers induce an inflammatory response along the interface and flap margin with the potential to cause diffuse lamellar keratitis (DLK)¹³. In thin flaps, DLK may increase the risk of flap perforation and necrosis. There were no cases of DLK in the present study, possibly because the FEMTO LDV Z8 laser uses low pulse energy; thus, it can lower an inflammatory response²⁷. In a previous study, DLK was more prevalent in procedures that used a high-pulse-energy laser than in those that used a low-pulse-energy laser.

Pulse rates and laser energy are key factors for creating the corneal flap in femtosecond LASIK. The femtosecond laser creates microplasma at the dissection plane that induces separation. High-pulse-energy femtosecond lasers may produce excessive gas bubbles, which can migrate from the pocket to the deep corneal tissue, prevent pupil tracking, and interfere with excimer laser ablation²⁸. Low-pulse-energy femtosecond lasers minimize gas bubbles, thereby reducing the incidence of gas bubble-related complications.

In the present study, elliptical flaps were created with the FEMTO LDV Z8 laser, which provides the additional advantage of improved gas dissipation. As the horizontal diameter of an elliptical flap is larger than its vertical diameter, the lamellar pocket space is located more peripherally than that of a circular flap, which allows for easier intraoperative release of gas¹⁷. Due to the low energy and creation of the venting channels associated with the FEMTO LDV Z8 laser, cuts were safely performed between depths of 85 and 100 μm minimize the risk of air penetration to the anterior chamber. The absence of gas-related complications in any of the subgroups in the present study may be attributed to the combination of a low-pulse-energy laser, venting channels, wider hinge angles, and the elliptical nature of the flap.

Furthermore, the inverted side cuts were wider at the base than at the epithelial surface. In an inverted side cut, the beveled edge of the flap is tucked under the lip of the peripheral stroma, thereby decreasing the possibility of postsurgical flap displacement²⁹. Corneal biomechanical properties are less affected by inverted side-cut angle flaps³⁰. Additionally, inverted side-cut flaps allow for better wound healing and improved apposition of severed nerves^{18,31}.

The biomechanical effect of flap creation on the residual stroma plays a critical role in the occurrence of unwanted complications such as ectasia^{32–34}. A sufficient RSBT after flap creation and excimer laser ablation reduce the likelihood of corneal ectasia³⁵. Due to the organization of the collagen lamellae, the anterior cornea is stronger than the posterior cornea, and in some situations, parts of the anterior third of the cornea can be preserved with a thinner flap, thereby retaining better biomechanics^{12,36,37}. Moreover, thin flaps preserve more residual stroma, which allows for the treatment of more severe myopia³⁸. Mathematical and theoretical models with higher RSBT have demonstrated favorable biomechanical changes in the underlying residual stroma, explaining the decreased risk of post-LASIK ectasia when the RSBT is higher^{29,32,36,39}.

In the present study, patients with a mean preoperative CCT of $556.04 \pm 31.04 \mu\text{m}$ (range: 486.0–612.0 μm) underwent thin-flap LASIK. LASIK flaps with thicknesses ranging between 80 and 100 μm resulted in good visual and refractive outcomes with no clinically relevant intraoperative or postoperative complications. This suggests that thin flaps can be considered even in eyes with higher pachymetry or in those requiring low amounts of ablation.

Our results demonstrate the clinical safety and efficacy of using low-pulse energy femtosecond lasers for creating elliptical thin-flaps in LASIK procedures. These findings build upon the earlier work by Cobo-Soriano et al. (2005), who analyzed thin-flap LASIK using mechanical microkeratomers. By employing femtosecond laser technology, we observed improved flap precision and consistency, which may contribute to better visual outcomes and reduced complications.

Limitations of this study include the retrospective nature of the study design and the short follow-up period (1 month), future studies. In addition, the subgroup sample sizes were not equally distributed. Future prospective studies will aim to include follow-up periods of at least 3 months to capture long-term outcomes and ensure comprehensive assessment of the refractive stability and safety, and compare these results with those from other thin flap (round) creation methods would be beneficial for more reliable findings.

Conclusion

In this study, an assessment of the clinical safety and efficacy of thin-flap OCT-guided LASIK using the low-pulse-energy FEMTO LDV Z8 femtosecond laser yielded promising results. Visual and refractive outcomes were comparable among the flap thickness subgroups, with flap thicknesses ranging from 85 to 100 μm . The achieved flap thicknesses were found to be highly predictable and consistent in all subgroups. Therefore, in the hands of an experienced surgeon, excellent safety, predictability, and efficacy in terms of visual outcomes with elliptical-shaped flaps are likely to be achieved.

Data availability

The datasets used and/or analyzed during the current study are available from the corresponding author on reasonable request.

Received: 11 December 2023; Accepted: 11 October 2024

Published online: 19 October 2024

References

- Liu, Y. C., Devarajan, K., Tan, T. E., Ang, M. & Mehta, J. S. Optical coherence tomography angiography for evaluation of reperfusion after pterygium surgery. *Am. J. Ophthalmol.* **207**, 151–158. <https://doi.org/10.1016/j.ajo.2019.04.003> (2019).
- Park, S. H. et al. Comparison of clinical outcomes after femtosecond laser in situ keratomileusis in eyes with low or high myopia. *Int. J. Ophthalmol.* **13**, 1780–1787. <https://doi.org/10.18240/ijo.2020.11.15> (2020).
- Abdel-Radi, M., Abdelmotaal, H. & Anwar, M. Thin-flap laser in situ keratomileusis-associated dry eye: a comparative study between femtosecond laser and mechanical microkeratome-assisted laser in situ keratomileusis. *Eye Contact Lens* **48**, 20–26. <https://doi.org/10.1097/ICL.0000000000000850> (2022).
- Vaddavalli, P. K. et al. Femtosecond laser-assisted retreatment for residual refractive errors after laser in situ keratomileusis. *J. Cataract Refract. Surg.* **39**, 1241–1247. <https://doi.org/10.1016/j.jcrs.2013.03.018> (2013).
- Pietila, J., Huhtala, A., Makinen, P. & Uusitalo, H. Flap characteristics, predictability, and safety of the Ziemer FEMTO LDV femtosecond laser with the disposable suction ring for LASIK. *Eye (Lond.)* **28**, 66–71. <https://doi.org/10.1038/eye.2013.244> (2014).
- Vryghem, J. C., Heireman, S. & Devogelaere, T. Thin-flap LASIK with a high-frequency, low-energy, small spot femtosecond laser – effectiveness and safety. *Eur. Ophthalmol. Rev.* **8**, 99–103. <https://doi.org/10.17925/EOR.2014.08.02.99> (2014).
- Huhtala, A., Pietila, J., Makinen, P. & Uusitalo, H. Femtosecond lasers for laser in situ keratomileusis: a systematic review and meta-analysis. *Clin. Ophthalmol.* **10**, 393–404. <https://doi.org/10.2147/OPHTH.S99394> (2016).
- Chua, D. et al. Eighteen-year prospective audit of LASIK outcomes for myopia in 53 731 eyes. *Br. J. Ophthalmol.* **103**, 1228–1234. <https://doi.org/10.1136/bjophthalmol-2018-312587> (2019).
- Kymionis, G. D. et al. Thin-flap laser in situ keratomileusis with femtosecond-laser technology. *J. Cataract Refract. Surg.* **39**, 1366–1371. <https://doi.org/10.1016/j.jcrs.2013.03.024> (2013).
- Giri, P. & Azar, D. T. Risk profiles of ectasia after keratorefractive surgery. *Curr. Opin. Ophthalmol.* **28**, 337–342. <https://doi.org/10.1097/ICU.0000000000000383> (2017).
- Melki, S. A. & Azar, D. T. LASIK complications: etiology, management, and prevention. *Surv. Ophthalmol.* **46**, 95–116. [https://doi.org/10.1016/s0039-6257\(01\)00254-5](https://doi.org/10.1016/s0039-6257(01)00254-5) (2001).
- Bages-Rousselon, Y. et al. Eighty-micron flap femtosecond-assisted LASIK for the correction of myopia and myopic astigmatism. *J. Cataract Refract. Surg.* **47**:445–449, DOI: (2021). <https://doi.org/10.1097/j.jcrs.0000000000000484> (2021).
- Chang, J. S. Complications of Sub-bowman's keratomileusis with a femtosecond laser in 3009 eyes. *J. Refract. Surg.* **24**, S97–S101. <https://doi.org/10.3928/1081597X-20080101-17> (2008).
- Steinert, R. F., Ashrafzadeh, A. & Hersh, P. S. Results of phototherapeutic keratectomy in the management of flap striae after LASIK. *Ophthalmology* **111**, 740–746. <https://doi.org/10.1016/j.ophtha.2003.06.015> (2004).
- Hatch, B. B., Moshirfar, M., Ollerton, A. J., Sikder, S. & Mifflin, M. D. A prospective, contralateral comparison of photorefractive keratectomy (PRK) versus thin-flap LASIK: assessment of visual function. *Clin. Ophthalmol.* **5**, 451–457. <https://doi.org/10.2147/OPHTH.S18967> (2011).
- Gupta, A. et al. Elliptical versus circular flap configuration in myopic eyes undergoing femtosecond laser in situ keratomileusis surgery: a contralateral eye study. *Ind. J. Ophthalmol.* **69**, 3457–3462. https://doi.org/10.4103/ijo.IJO_836_21 (2021).
- Lin, H. Y. et al. Influences of flap shape and hinge angle on opaque bubble layer formation in femtosecond laser-assisted LASIK surgery. *J. Refract. Surg.* **33**, 178–182. <https://doi.org/10.3928/1081597X-20161219-02> (2017).
- Taha, S., Azzam, S., Anis, M., Zaaouz, C. & Hosny, M. Verification and measurement of the side-cut angle of corneal flap in patients undergoing LASIK surgery using FS 200 kHz femtosecond laser system versus conventional mechanical microkeratome. *Clin. Ophthalmol.* **13**, 985–992. <https://doi.org/10.2147/OPHTH.S201150> (2019).
- Knox Cartwright, N. E., Tyrer, J. R., Jaycock, P. D. & Marshall, J. Effects of variation in depth and side cut angulations in LASIK and thin-flap LASIK using a femtosecond laser: a biomechanical study. *J. Refract. Surg.* **28**, 419–425. <https://doi.org/10.3928/1081597X-20120518-07> (2012).
- Cummings, A. B., Cummings, B. K. & Kelly, G. E. Predictability of corneal flap thickness in laser in situ keratomileusis using a 200 kHz femtosecond laser. *J. Cataract Refract. Surg.* **39**, 378–385. <https://doi.org/10.1016/j.jcrs.2012.10.041> (2013).
- Tomita, M. et al. Evaluation of LASIK treatment with the Femto LDV in patients with corneal opacity. *J. Refract. Surg.* **28**, 25–30. <https://doi.org/10.3928/1081597X-20111213-01> (2012).
- Vryghem, J. C., Devogelaere, T. & Stodulka, P. Efficacy, safety, and flap dimensions of a new femtosecond laser for laser in situ keratomileusis. *J. Cataract Refract. Surg.* **36**, 442–448. <https://doi.org/10.1016/j.jcrs.2009.09.030> (2010).
- Liu, C. H. et al. Opaque bubble layer: incidence, risk factors, and clinical relevance. *J. Cataract Refract. Surg.* **40**, 435–440. <https://doi.org/10.1016/j.jcrs.2013.08.055> (2014).
- Asshauer, T., Latz, C., Mirshahi, A. & Rathjen, C. Femtosecond lasers for eye surgery applications: historical overview and modern low pulse energy concepts. *Adv. Opt. Technol.* **10**, 393–408. <https://doi.org/10.1515/aot-2021-0044> (2021).
- Mudarisov, B. et al. Safety and precision of two different flap-morphologies created during low energy femtosecond laser-assisted LASIK [Poster Presentation], ESCRS 8–11 (Amsterdam, 2021).
- Probst, L. E. & Machat, J. Removal of flap striae following laser in situ keratomileusis. *J. Cataract Refract. Surg.* **24**, 153–155. [https://doi.org/10.1016/s0886-3350\(98\)80193-4](https://doi.org/10.1016/s0886-3350(98)80193-4) (1998).
- Tomita, M., Sotoyama, Y., Yukawa, S. & Nakamura, T. Comparison of DLK incidence after laser in situ keratomileusis associated with two femtosecond lasers: Femto LDV and IntraLase FS60. *Clin. Ophthalmol.* **7**, 1365–1371. <https://doi.org/10.2147/OPHTH.S47341> (2013).
- Lim, D. H. et al. Incidence and risk factors of opaque bubble layer formation according to flap thickness during 500-kHz FS-LASIK. *J. Refract. Surg.* **35**, 583–589. <https://doi.org/10.3928/1081597X-20190814-01> (2019).
- Wei, C. H., Mei, L. X., Ge, Y. & Zhang, P. F. Managements of vertical gas breakthrough in femtosecond laser assisted LASIK. *Int. J. Ophthalmol.* **13**, 1503–1504. <https://doi.org/10.18240/ijo.2020.09.25> (2020).
- Li, H. et al. Comparison of the effects of different side-cut angles on corneal biomechanical properties after femtosecond laser assisted-laser in situ keratomileusis. *Zhonghua Yan Ke Za Zhi.* **53**, 23–32. <https://doi.org/10.3760/cma.j.issn.0412-4081.2017.01.006> (2017).
- Jhanji, V. et al. Conventional versus inverted side-cut flaps for femtosecond laser-assisted LASIK: laboratory and clinical evaluation. *J. Refract. Surg.* **33**, 96–103. <https://doi.org/10.3928/1081597X-20161102-02> (2017).
- Khamar, P. et al. Biomechanics of LASIK flap and SMILE cap: a prospective, clinical study. *J. Refract. Surg.* **35**, 324–332. <https://doi.org/10.3928/1081597X-20190319-01> (2019).
- Medeiros, F. W., Sinha-Roy, A., Alves, M. R. & Dupps, W. J. Biomechanical corneal changes induced by different flap thickness created by femtosecond laser. *Clin. (Sao Paulo)* **66**, 1067–1071. <https://doi.org/10.1590/S1807-59322011000600025> (2011).

34. Ong, H. S. et al. Corneal ectasia risk and percentage tissue altered in myopic patients presenting for refractive surgery. *Clin Ophthalmol.* **13**, 2003–2015. <https://doi.org/10.2147/OPTH.S215144> (2019).
35. Azar, D. T. et al. Thin-flap (sub-bowman keratomileusis) versus thick-flap laser in situ keratomileusis for moderate to high myopia: case-control analysis. *J. Cataract Refract. Surg.* **34**, 2073–2078. <https://doi.org/10.1016/j.jcrs.2008.08.019> (2008).
36. Randleman, J. B., Dawson, D. G., Grossniklaus, H. E., McCarey, B. E. & Edelhauser, H. F. Depth-dependent cohesive tensile strength in human donor corneas: implications for refractive surgery. *J. Refract. Surg.* **24**, S85–S89. <https://doi.org/10.3928/1081597X-20080101-15> (2008).
37. Muller, L. J., Pels, E. & Vrensen, G. F. The specific architecture of the anterior stroma accounts for maintenance of corneal curvature. *Br. J. Ophthalmol.* **85**, 437–443. <https://doi.org/10.1136/bjo.85.4.437> (2001).
38. Lim, D. H. et al. Prospective contralateral eye study to compare 80- and 120-mum flap LASIK using the VisuMax femtosecond laser. *J. Refract. Surg.* **29**, 462–468. <https://doi.org/10.3928/1081597X-20130617-04> (2013).
39. Reinstein, D., Archer, Z., J. T., Gobbe, M. & Johnson, N. Accuracy and reproducibility of Artemis central flap thickness and visual outcomes of LASIK with the Carl Zeiss Meditec VisuMax femtosecond laser and MEL 80 excimer laser platforms. *J. Refract. Surg.* **26**, 107–119. <https://doi.org/10.3928/1081597X-20100121-06> (2010).

Acknowledgements

The authors declare no competing interests.

Author contributions

Conceptualization: H.L., Y.C.; Formal Analysis: H.L., Y.C., W.C.; Investigation: H.L., Y.C., W.C., P.L.; Methodology: H.L., Y.C.; Project administration: H.L., Y.C., P.L.; Validation: H.L., Y.C., W.C.; Writing—original draft: H.L., Y.C., P.L.; Writing—reviewing & editing: H.L., Y.C., P.L.

Funding

This research did not receive any specific grant from funding agencies in the public, commercial, or not-for-profit sectors.

Competing interests

The authors declare no competing interests.

Additional information

Correspondence and requests for materials should be addressed to Y.-J.C.

Reprints and permissions information is available at www.nature.com/reprints.

Publisher's note Springer Nature remains neutral with regard to jurisdictional claims in published maps and institutional affiliations.

Open Access This article is licensed under a Creative Commons Attribution-NonCommercial-NoDerivatives 4.0 International License, which permits any non-commercial use, sharing, distribution and reproduction in any medium or format, as long as you give appropriate credit to the original author(s) and the source, provide a link to the Creative Commons licence, and indicate if you modified the licensed material. You do not have permission under this licence to share adapted material derived from this article or parts of it. The images or other third party material in this article are included in the article's Creative Commons licence, unless indicated otherwise in a credit line to the material. If material is not included in the article's Creative Commons licence and your intended use is not permitted by statutory regulation or exceeds the permitted use, you will need to obtain permission directly from the copyright holder. To view a copy of this licence, visit <http://creativecommons.org/licenses/by-nc-nd/4.0/>.

© The Author(s) 2024